Laser and Particle Beams (2006), *24*, 241–247. Printed in the USA.

DOI: 10.1017/S0263034606060356

Laser-induced plasma spectroscopy for mine detection and verification

WOLFGANG SCHADE, CHRISTIAN BOHLING, KONRAD HOHMANN, AND DIRK SCHEEL
Technische Universität Clausthal, Institut für Physik und Physikalische Technologien, Clausthal, Germany

(RECEIVED 1 February 2005, ACCEPTED 15 November 2005)

Abstract

Laser-induced breakdown spectroscopy (LIBS) in combination with a conventional mine prodder is applied for remote detection of explosives and mine housing materials. High power subnanosecond laser pulses (pulse power $E_p = 0.6$ mJ and pulse duration $\Delta t = 650$ ps) at 1064 nm with a typical repetition rate of 10 kHz are generated by using a passively Q-switched Cr^{4+}:Nd^{3+}:YAG microchip-laser as seed-laser for an Yb-fiber amplifier. In the present investigation, the ratios of "late" and "early" LIBS intensities for the cyanide (CN) plasma emission at 388 nm and for the C-emission at 248 nm are used for data analysis. This allows the classification of different explosives and mine casing materials under real time conditions and also similar applications to materials processing.

Keywords: Explosives; Fiber laser; Laser spectroscopy; LIBS; Mines

1. INTRODUCTION

The development of novel online and insitu methods for the classification of materials is still an important field of research in different disciplines, such as industrial process control and environmental diagnostics. In this context, characterization of explosives and housing materials for mine detection applications, but also for anti-terror purposes is still very critical. The UNO estimated worldwide between 60 and 100 millions of mines that have to be detected and then destroyed. Each year about 25000 people are involved in accidents caused by mines (Altmann, 2001). Special danger comes from mines that are housed by plastic materials and therefore cannot be detected by conventional geo-radar or metal detection methods.

Optical methods are very promising because they operate in non-contact, they are very sensitive, give real-time results, and in most cases, there is no need for sample preparation. When using miniaturized laser sources and fiber optics laser spectroscopy offers the possibility to develop compact laser sensors for various analytical applications. In this context, laser-induced breakdown spectroscopy (LIBS) is very interesting, because this method allows analyzing solid state samples in a real-time operation mode (Sattmann *et al*., 1998; Wainner *et al*., 2001; Lancaster *et al*., 1999; Bublitz *et al*., 2001). This is highlighted in this paper, for the characterization of explosives in different environments with special emphasis on the detection of hidden explosives, for example, improving conventional mine detection prodder by using the LIBS technique.

A nonmagnetic mine prodder is designed for manually locating anti-personnel mines that are buried at depths up to 0.25 m. The device consists of three main components, a handle, an extension tube, and the probe itself. Typical operational modes are kneeling or upright position of the operator while carefully digging in the soil. The prodder itself is a lightweight and robust tool; objects in the soil are tracked down by direct contact with the probe. The objective of this investigation is to improve the mine prodder by adoption of laser and fiber technology without much change in the conventional handling of the device.

LIBS are not only a tool for diagnostics but also for material processing. Therefore, laser drilling and online diagnostics of the material processed can be achieved if the laser power is sufficiently high as demonstrated recently in many cases (Fernandez *et al*., 2005; Trusso *et al*., 2005; Gamaly *et al*., 2005; Gavrilov *et al*., 2004; Mulser & Schneider, 2004).

The output power of a microchip-laser at 1064 nm can be amplified by a factor up to 100, when using an Ytterbium-fiber amplifier system, resulting in a peak power of several MW. Such power levels allow drilling a hole through

Address correspondence and reprint requests: Wolgang Schade, Technische Universität Clausthal, Institut für Physik und Physikalische Technologien, Leibnizstrasse 4, Clausthal D-38678, Germany. E-mail: wolfgang.schade@tu-clausthal.de

the housing of a mine or a suitcase, and simultaneously analyzing the material processed, as well as the inner material by means of LIBS. In the case of energetic materials, this can be done without ignition of explosives when applying power levels below 400 mJ/pulse.

2. FIBER OPTIC LIBS: SENSOR

2.1. LIBS Basics

In general, the atomic composition of explosives, plastics, and soil is given by the following elements: carbon (C), nitrogen (N), oxygen (O), and hydrogen (H) (Fig. 1). When focusing an intense pulsed laser ($\lambda = 1064$ nm, $\Delta t < 1$ ns, $E_p > 0.1$ mJ) on the surface to be investigated, plasma will be generated instantaneously. Surface molecules are fragmented into their atomic compounds and excited atoms, molecules and molecular compounds, as well as electrons generated by the plasma. When the laser pulse is off, no energy is transferred to the sample, and the ions and electrons recombine as well as the excited states, which results in the emission of light. In Figure 2, the temporal evolution of laser-induced plasma is shown schematically. Spectrally-resolved detection of the plasma emission gives information on the atomic composition of the sample ("first order fingerprint"). This can be used for characterization of different samples, if the atomic composition is different from the sample being sampled. Plastics and explosives are composed of the same elements, and therefore, cannot be classified by only measuring the LIBS intensities. However, when using the temporal evolution of the LIBS intensities for specific wavelengths, a data analysis can be developed that allows a selective sample analysis. Depending on the absorption cross-section for the materials under investigation, the laser-induced plasma temperature is different for different materials. Plasma temperatures up to 12000 K are obtained when using laser pulses of a few mJ. This effect results in characteristic LIBS intensity decay times for different materials. The decay times are typically in the order of several tens to a few hundreds of nanoseconds ("second order fingerprint") depending on the applied laser power and the material to be analyzed.

To investigate these effects in detail, the fundamental output of a diode laser pumped and passively Q-switched

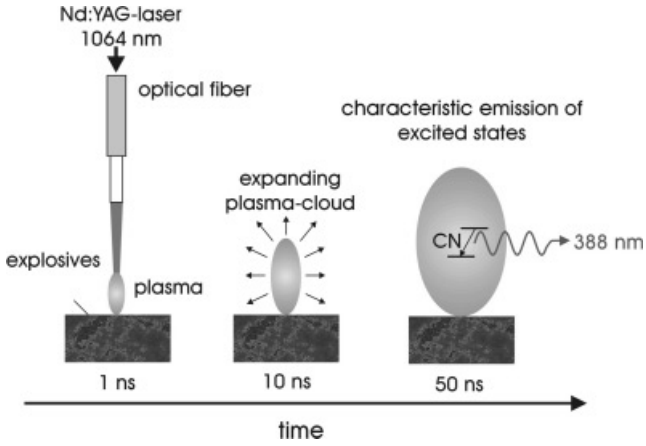

Fig. 2. Time-evolution of LIBS.

Cr^{4+}:Nd^{3+}:YAG microchip-laser (Zayhowski, 1996; Voss *et al.*, 2001) (pulse duration $\Delta t \leq 1$ ns, pulse repetition rate $\nu = 200$ Hz, pulse energy $E_p = 0.4$ mJ, emission wavelength $\lambda = 1064$ nm (Alphalas GmbH, Göttingen, Germany)) is focused on the surface of the sample under investigation (diameter $d \approx 200$ μm). Then plasma is generated. The LIBS emission is recorded by a gateable optical multichannel analyzer (OMA-4 system, EG&G, time-resolution $>$ 5 ns). The plasma emission is measured at 388 and 248 nm, which is attributed to cyanide (CN) and atomic carbon. Temporal- and spectrally-resolved LIBS spectra are shown in Figure 3 for trinitrotoluene (TNT) (a), for the plastic polyamide (b), as well as the LIBS intensity decay for the CN-line at 388 nm for TNT (c), and polyamide (d). The strong carbon emission is because of the relatively high amount of carbon in these materials, but the CN emission is explained by a reaction of the carbon emitted from the material and the nitrogen from the ambient air, which is also ionized by the plasma. If the experiments are performed under vacuum conditions, the C-emission is still present, but the CN-emission at 388 nm vanishes. Also the polyamide spectrum (Fig. 3c) shows calcium (CA) contaminations of the plastic material around 390 nm that easily can be detected simultaneously by the LIBS technique.

In conclusion, time-resolved recording of LIBS intensities for the C- or the CN-plasma emission after excitation with short laser pulses ($\Delta t < 1$ ns), allows the classification

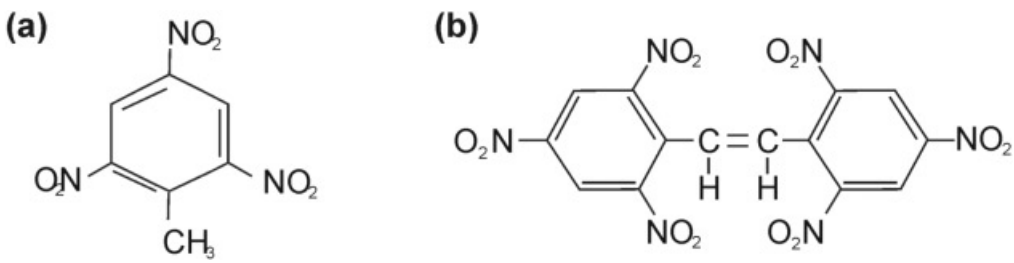

Fig. 1. Atomic composition of two explosives (**a**) TNT (trinitrotoluene) and (**b**) HNS (hexanitrostilbene).

https://doi.org/10.1017/S0263034606060356 Published online by Cambridge University Press

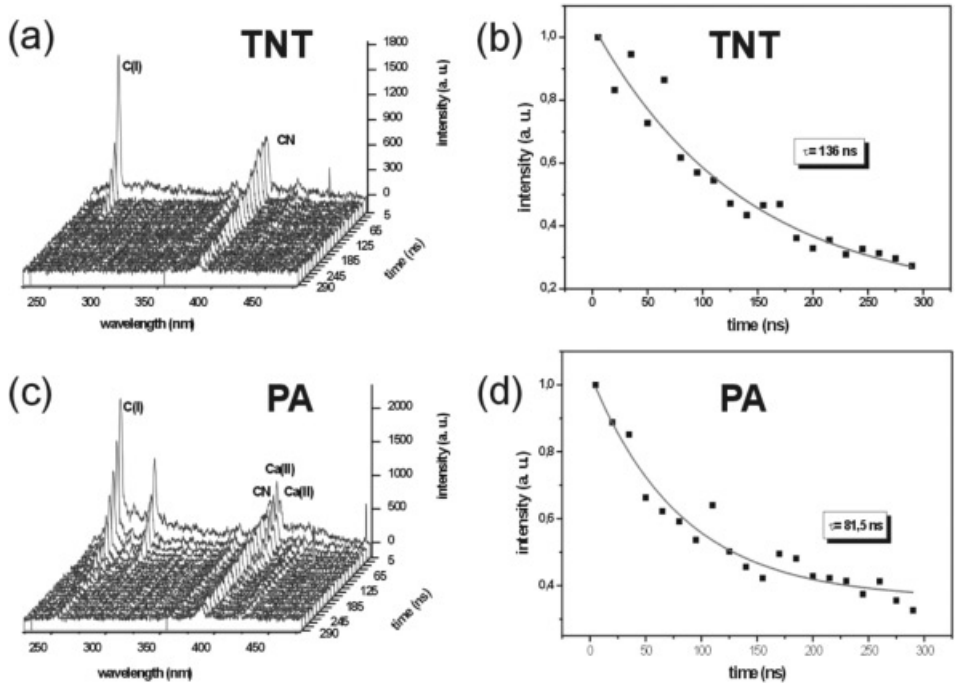

Fig. 3. Time- and spectrally resolved LIBS intensity spectra of TNT (**a**) and polyamide (**b**). The decay of the CN-intensity at 388 nm is analyzed for TNT (**c**) and polyamide (**d**). When fitting single exponentials to the data points decay times $\tau = 136$ ns and $\tau = 81.5$ ns are obtained for trinitrotoluene (TNT) and polyamide (PA). The laser excitation was at 1064 nm and the pulse power about 5 mJ.

of different explosives and plastics even though the atomic composition of the material is the same. In the case of explosives, no ignition of the material is obtained for pulse energies up to 400 mJ. In Figure 3b and Figure 3d, the estimated 1/e plasma decay times for the CN-emission (388 nm) are shown for TNT and the plastic material (PA), respectively. In a first order approximation, the plasma intensity decay can be described by a single exponential. Therefore, single exponentials are fitted to the data points resulting in decay times $\tau = 136$ ns and $\tau = 81.5$ ns for TNT and PA, respectively. In Table 1, LIBS decay times for laser excitation at 1064 nm and observation wavelengths 248 nm (CI) and 388 nm (CN) are summarized for different materials. When storing such data on a microcomputer, they can be used for online and insitu characterization of samples by comparing them with real time LIBS measurements (Romano *et al*., 2004; Schade *et al*., 2004).

Table 1. *Summary of LIBS 1/e decay times for different materials and fixed experimental conditions*

Laser	Nd:YAG (1064 nm)	Nd:YAG (1064 nm)
Line (nm)	CN (388 nm)	C (247.9 nm)
Decay time		
TNT	136 ns	15.4 ns
HNS	185 ns	18.1 ns
PA	81 ns	47.8 ns
PVC	140 ns	33.1 ns

2.2. Miniaturized Laser for LIBS Applications

The development of smart, portable, and rugged LIBS fiber optic sensors, for example, upgrade for a conventional mine prodder or as a sensor for the detection of hidden explosives in anti-terror purposes, requires the supply of a powerful and miniaturized laser source. This is done in this investigation by applying a passively Q-switched Cr^{4+}:Nd^{3+}:YAG laser as a seed laser for a fiber amplifier. The Cr-ions in the laser crystal, act as a passive Q-switch. Therefore, when pumping the Cr^{4+}:Nd^{3+}:YAG laser crystal (Stankov, J. 2002, private communication) with a continuous wave (cw) diode laser (λ = 808 nm, P = 2 W), the microchip-laser emits pulses below 700 ps in duration, a repetition rate of up to 20 kHz, and a pulse energy of up to 25 μJ. In Figure 4, the set-up for a microchip-laser as used in this investigation (a) together with the temporal profile of a single pulse (b), the change of the repetition rate dependence on the laser current (c) and the pulse to pulse stability (d) are shown. For amplification of the microchip-laser output, an Ytterbium fiber amplifier (Höfer *et al*., 2001; Limpert *et al*., 2001), which is also pumped by a high power cw diode laser (P = 50 W, λ = 976 nm) is used (Fig. 5a). The microchip-laser operates as a seed-laser and pulse amplification with a factor of up to 100 is possible (Geiser *et al*., 2004). This gives a

https://doi.org/10.1017/S0263034606060356 Published online by Cambridge University Press

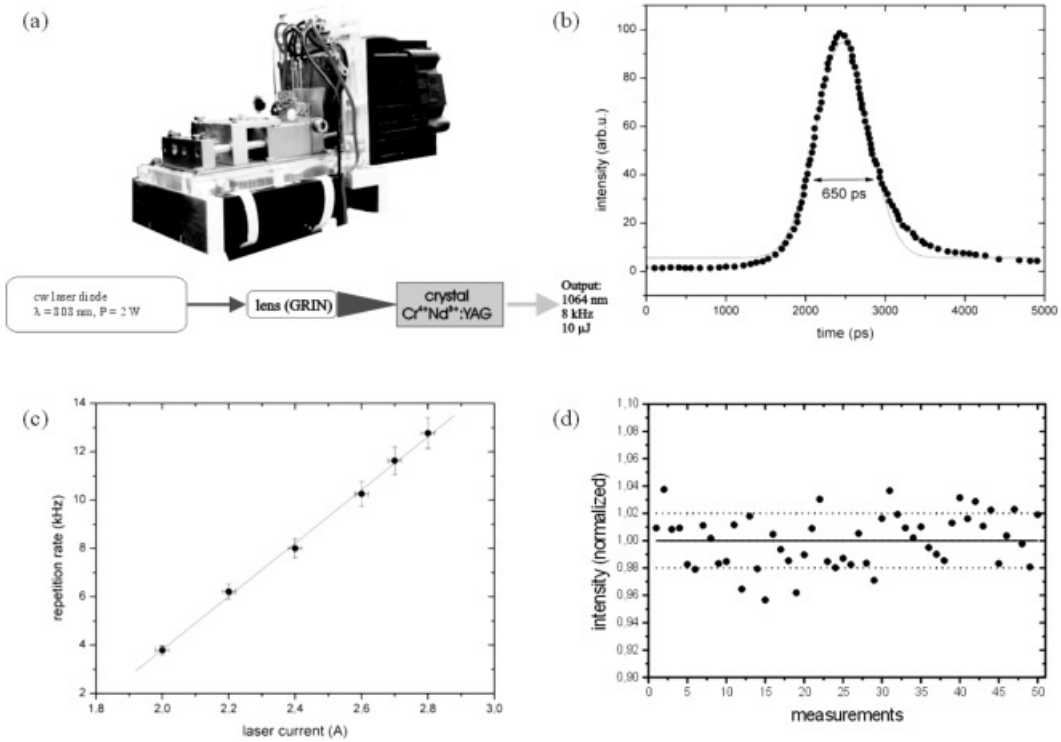

Fig. 4. (**a**) Schematic and photo of a passively Q-switched Cr^{4+}:Nd^{3+}:YAG microchip laser, (**b**) temporal pulse shape, (**c**) variation of repetition rate, and (**d**) pulse to pulse stability.

peak power in the order of a few MW at the laser wavelength 1064 nm, which allows drilling holes into the housing of plastic mines (Fig. 5b), and synchronously monitoring the material characteristics by time-resolved recording of LIBS intensities.

3. LIBS CLASSIFICATION OF MATERIALS

With respect to practical applications as a fiber optic laser sensor, for example, for mine detection, the time-resolved LIBS method is simplified, such as LIBS intensities in two time windows, with respect to the laser pulse recorded. Then, the ratio of these intensities is calculated and used as a measure for the classification of the material to be investigated. The first time window opens directly after the laser pulse for a typical duration of 50 ns ("early LIBS intensity"), while the second is activated with a delay of 50 ns with respect to the laser pulse for a duration of 200 ns ("late LIBS intensity"). For fixed excitation conditions (diameter laser spot on surface, pulse power), the ratio of "late" to

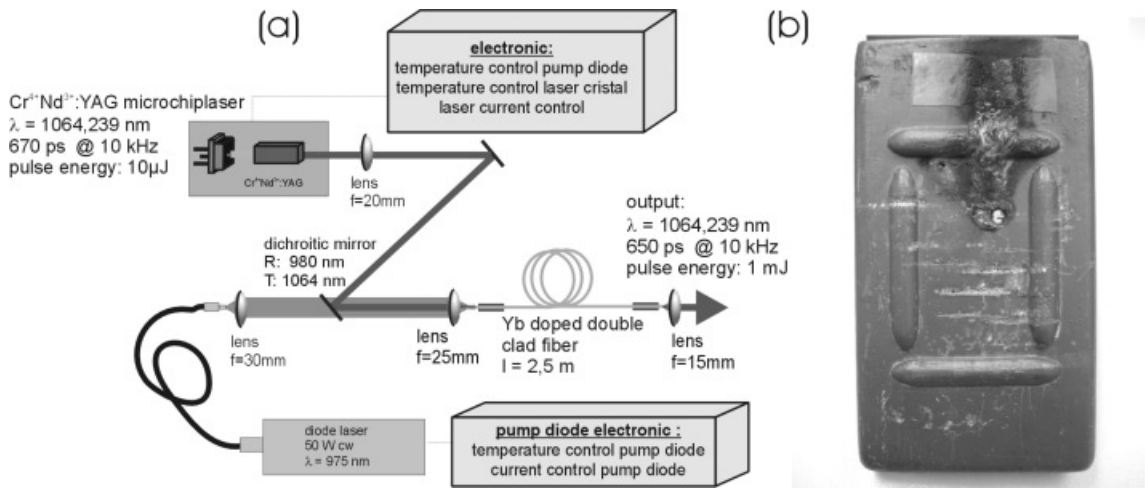

Fig. 5. (**a**) Yb-fiber amplifier with $Cr^{3+}Nd^{4+}$:YAG microchip laser as seed-laser. (**b**) Drilling holes into the casing of a plastic mine.

https://doi.org/10.1017/S0263034606060356 Published online by Cambridge University Press

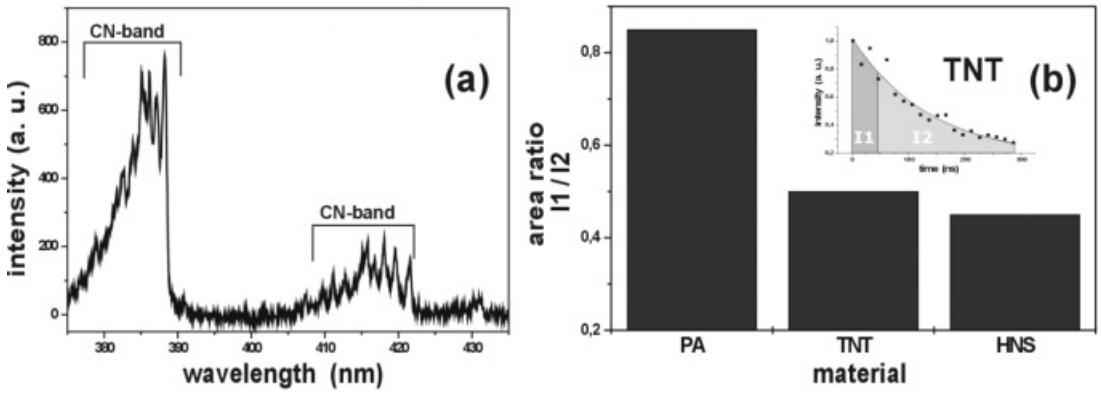

Fig. 6. (**a**) CN-emission of the explosive TNT. (**b**) Time-integrated ratios of "early" and "late" LIBS intensities ("area ratio") for different materials and laser excitation at 1064 nm.

"early" LIBS intensities for C- or CN-emission is a characteristic measure for different materials. This is shown in Figure 6 when recording the CN-emission and different materials.

In Figure 6a, the spectrum of the CN emission is shown for the explosive TNT in the spectral range of 350 to 440 nm with an intensity maximum at 388 nm. Figure 6b shows the measured ratios of "late" to "early" LIBS intensities ("area ratio") for two explosives TNT and HNS and polyamide. The results show that different materials can be classified by time-integrated LIBS, even though the material composition consists of the same elements. The accuracy of the classification strongly depends on the experimental parameters, especially the temporal setting of the integration windows. These parameters need to be determined accurately in laboratory experiments to optimize the sensitivity of the method, and then stored in a database. A set-up as used in the first practical applications for the characterization of explosives and mine casings is shown in Figure 7a. A photo of a laser induced plasma directly in front of a laser mine prodder on a TNT sample is shown in Figure 7b. The accuracy of the fiber optic laser prodder is optimized when using self-learning neuronal networks for real-time data analysis. Then the intensity of the LIBS signal, the time evolution, and the "area ratio" are used for classification. As an example, the system acquires this data by analyzing the time-evolution of CN-plasma emission for one sample under investigation, this information is stored in a 10×10 matrix, for example, on position 2×10 (Fig. 7c). Then the next sample is analyzed by the same procedure. The system compares the result with all previous measurements, if it is identical, it is stored on the same matrix element, if not, and a new element is generated. In such a way, 100 different samples can be classified when using a 10×10 matrix as discussed in this paper. When calibrating the system with reference data from well known mine casing materials, for example, the matrix element 2×10 can be identified as mine casing material of type y.

By this miniaturization of lasers and the application of fiber optics, the LIBS method can easily be integrated into a conventional mine prodder to improve the conventional mine searching process, but the same method can also be applied for the detection and verification of explosives in hidden environments, such as suitcases or any type of luggage, which will be interesting for fighting terror attacks, for example, at airports or any public location.

4. SUMMARY

The results show that samples with same atomic composition (for example, C, N, O, and H), can be classified with sufficiently high accuracy by recording LIBS intensities for CN- or C-emission in two different time windows, with respect to the exciting laser pulse followed by real-time data analysis, using the self-learning neuronal networks. The practical capability of the method is demonstrated as different explosives such as TNT, HNS, H5, or tetryl, but also plastic materials such as PVC or PA are analyzed. Beside classification of materials, contaminations in materials can be monitored by this technique. An example is the detection of CA contaminations in explosives, for example, in HNS but also in PA. Here CA is introduced during material processing. Therefore, the detection of impurities in materials may give important hints from the history of the material itself. Mine casing materials are investigated and can be classified by the same method.

The use of miniaturized and powerful lasers for the generation of plasma and fiber optics offer new and very interesting fields of applications: The integration of a LIBS sensor into a conventional mine prodder or the online and insitu detection of hidden explosives. In both cases, real-time information is achieved and the analysis is performed in non-contact modus. This will be very important in order to improve safety aspects and the speed for analysis for clearing mines.

https://doi.org/10.1017/S0263034606060356 Published online by Cambridge University Press

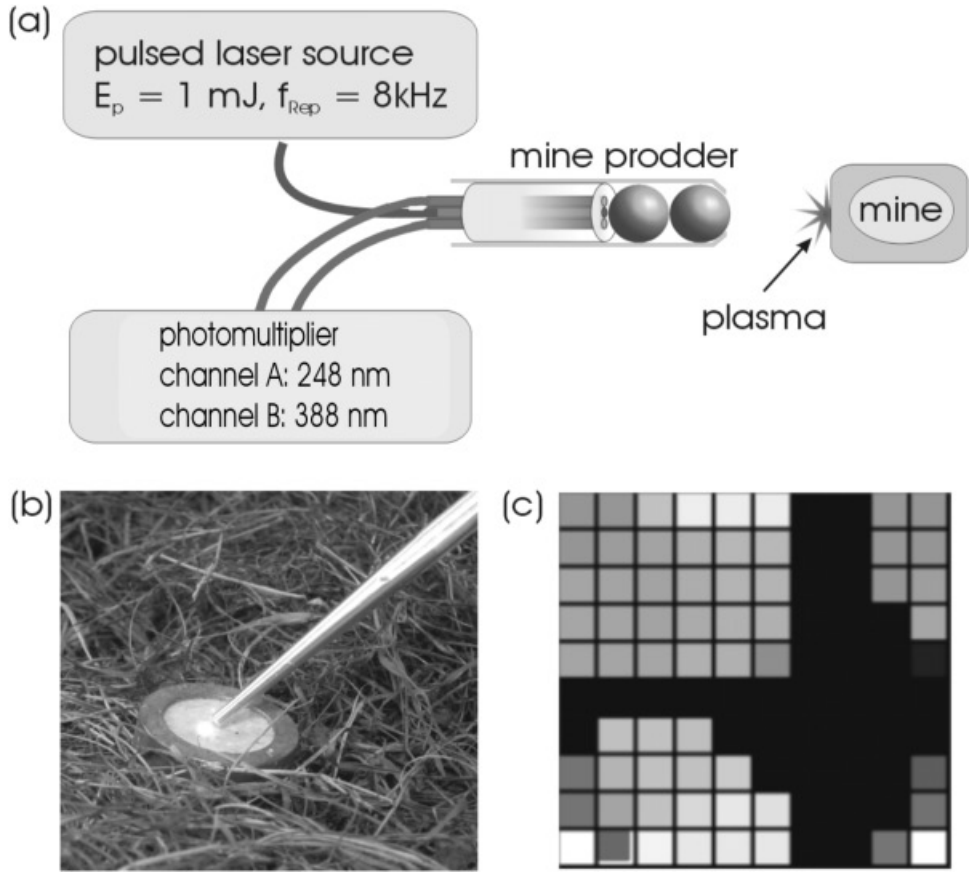

Fig. 7. (**a**) Configuration of a LIBS-based mine detection needle for online and insitu classification of explosives. (**b**) Photo of a laser induced plasma on TNT directly in front of the laser prodder. (c) Map of neurons for material classification when using self learning neuronal networks for real-time data analysis.

ACKNOWLEDGMENT

Financial support by the German Ministry of Defense under contract No. 005/B-3D023/X5165 is gratefully acknowledged.

REFERENCES

Altmann, J. (2001). Neue Technologien für die Minensuche. *Physik in unserer Zeit* **32**, 26–32.

Bublitz, J., Dölle, C., Schade, W., Hartmann, A. & Horn, R. (2001). Laser-induced breakdown spectroscopy for soil diagnostics. *Euro J. Soil Sci.* **52**, 305–312.

Fernandez, J.C., Hegelich, B.M., Cobble, J.A., Flippo, K.A., Letzring, S.A., Johnson, R.P., Gautier, D.C., Shimada, T., Kyrala, G.A., Wang, Y.Q., Wetteland, C.J. & Schreiber, J. (2005). Laser-ablation treatment of short-pulse laser targets: Toward an experimental program on energetic-ion interactions with dense plasmas. *Laser Part. Beams* **23**, 267–273.

Gamaly, E.G., Luther-Davies, B., Kolev, V.Z., Madsen, N.R., Duering, M. & Rode, A.V. (2005). Ablation of metals with picosecond laser pulses: Evidence of long-lived non-equilibrium surface states. *Laser Part. Beams* **23**, 167–176.

Gavrilov, S.A., Golishnikov, D.M., Gordienko, V.M., Savel'ev, A.B. & Volkov, R.V. (2004). Efficient hard X-ray source using femtosecond plasma at solid targets with a modified surface. *Laser Part. Beams* **22**, 301–306.

Geiser, P., Bohling, C., Willer, U., Schade, W., Reich, M. & Tünnermann, A. (2004). A pulsed laser-source for MIR-LIDAR. Conference on Lasers and Electro-optics. San Francisco: CTuP57.

Höfer, S., Liem, A., Limpert, J., Zellmer, H., Tünnermann, A., Unger, S., Jetschke, S., Müller H.R. & Freitag, I. (2001). Single-frequency master-oscillator fiber power amplifier system emitting 20 W of power. *Opt. Lett.* **26**, 1326–1328.

Lancaster, D.E., McNesby, K.L., Daniel, R.G. & Miziolek, A.W. (1999). Spectroscopic analysis of fire suppressants and refrigerants by laser induced breakdown spectroscopy. *Appl. Opt.* **38**, 1476–1480.

Limpert, J., Liem, A., Gabler, T., Zellmer, H., Tünnermann, A., Unger, S., Jetschke, S. & Müller, H.R. (2001). High-average power picosecond Yb-doped fiber amplifier. *Opt. Lett.* **26**, 1849–1851.

Mulser, P. & Schneider, R. (2004). On the inefficiency of hole boring in fast ignition. *Laser Part. Beams* **22**, 157–162.

Romano, C., Gräser, S., Faulian, K., Schade, W. & Holl, G. (2004). *Application of LIBS Spectroscopy for Remote Bulk Detection of Explosives. Detection of Bulk Explosives* (Schubert, H. and Kuznetsov, A, Eds.), pp. 167–173. Netherlands: Kluwer Academic Publishers.

Sattmann, R., Mönch, I., Krause, H., Noll, R., Couris, S., Hatziapostolou, A., Mavromanolakis, A., Fotakis, C., Larrauri, E. & Miguel, R. (1998). Laser-induced break-

https://doi.org/10.1017/S0263034606060356 Published online by Cambridge University Press

down spectroscopy for polymer identification. *Appl Spectro.* **52**, 456–461.

Schade, W., Holl, G., Holl, A. & Bublitz, J. (2004). European Patent EP 1 443 319 A1.

Trusso, S., Barletta, E., Barreca, F., Fazio, E. & Neri, F. (2005). Time resolved imaging studies of the plasma produced by laser ablation of silicon in O-2/Ar atmosphere. *Laser Part. Beams* **23**, 149–153.

Voss, T., Scheel, D. & Schade, W. (2001). A microchip-laser-pumped DFB polymer-dye laser. *Appl. Phys. B* **73**, 105–109.

Wainner, R.T., Harmon, R.S., Miziolek, A.W., McNesby, K.L. & French, P.D. (2001). Analysis of environmental lead contamination. *Spectrochim. Acta. B.* **56**, 777–793.

Zayhowski, J.J. (1996). Ultraviolet generation with passively Q-switched microchip lasers. *Opt. Lett.* **21**, 588–590.

https://doi.org/10.1017/S0263034606060356 Published online by Cambridge University Press